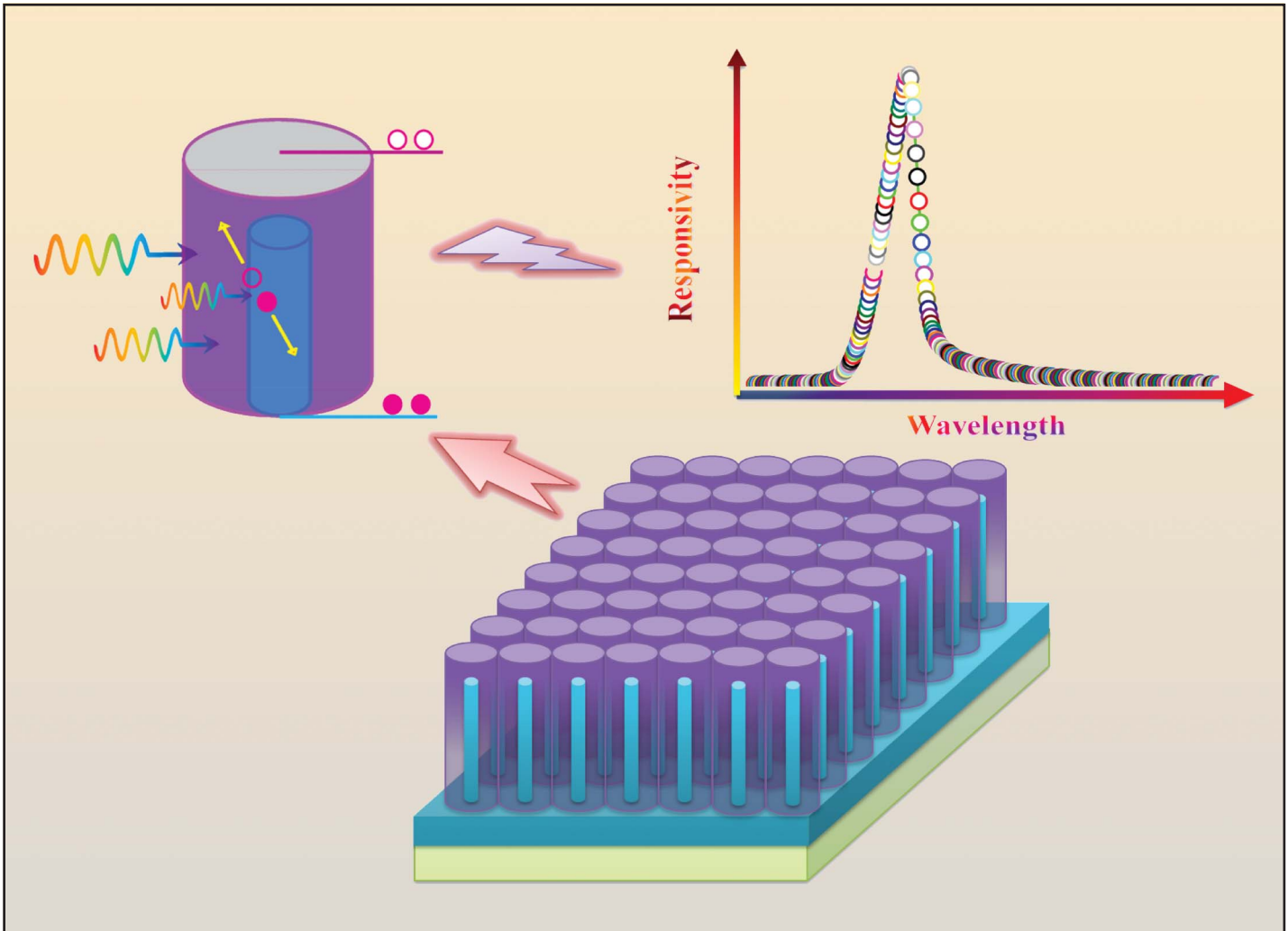

The work was carried out in the Changchun Institute of Optics, Fine Mechanics and Physics, Chinese Academy of Sciences, Changchun, China.

Title: Self-powered spectrum-selective photodetectors fabricated from n-ZnO/p-NiO core–shell nanowire arrays

Ultraviolet photodetectors have been fabricated from n-ZnO/p-NiO core–shell nanowire arrays, the photodetectors can work without an external power source, and show a response only to a narrow spectrum region.

As featured in:

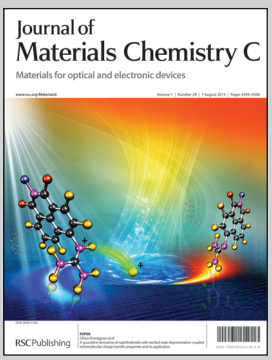

See P.-N. Ni *et al.*,
J. Mater. Chem. C, 2013, **1**, 4445.

RSC Publishing

www.rsc.org/MaterialsC

Registered Charity Number 207890

Journal of Materials Chemistry C

RSC Publishing

PAPER

Self-powered spectrum-selective photodetectors fabricated from n-ZnO/p-NiO core–shell nanowire arrays

Cite this: J. Mater. Chem. C, 2013, 1, 4445

Pei-Nan Ni,[ab] Chong-Xin Shan,*[a] Shuang-Peng Wang,[a] Xing-Yu Liu[ab] and De-Zhen Shen*[a]

Received 20th March 2013
Accepted 20th May 2013

DOI: 10.1039/c3tc30525b

www.rsc.org/MaterialsC

Self-powered, highly spectrum-selective photodetectors have been fabricated from n-ZnO/p-NiO core–shell nanowire arrays. In the structure, the outer-layer of the p-NiO acts as a "filter" which can filter out the photons with short wavelength. In this way, highly spectrum-selective photodetectors that only respond to a narrow spectrum range have been obtained.

Introduction

Quasi-one-dimensional (quasi-1D) core–shell semiconductor nanostructures have received considerable attention as building blocks for optoelectronic devices.[1–3] It has been demonstrated that quasi-1D structures have many advantages over conventional planar devices, and they have proved to be a promising choice for solar cells and photodetectors (PDs).[4–9] Specifically, the large surface-to-volume ratio as well as the low reflectance due to light scattering and trapping helps to increase the collection efficiency of photons.[10,11] Furthermore, the core–shell structures afford a direct electrical pathway for the photogenerated carriers to transport to the corresponding electrodes rapidly, which is favorable for reducing the nonradiative recombination and carrier scattering loss.[12,13] So far, remarkable photoresponse characteristics have been studied and great progress has been made through the state-of-the-art research activities that focus on nanostructures, such as ZnO, ZnS, V_2O_5, ZrS_2, Sb_2Se_3, CdS, CdSe, InGaAs, *etc.*[14–16] However, since photons with energy larger than the bandgap will be absorbed by the semiconductor and contribute to the response, this kind of nanoscale semiconductor PDs usually show response to a broad spectrum region,[17–19] that is to say, their spectrum-selectivity is quite poor, which restricts the potential applications of such PDs in monitoring a very narrow spectrum range.

Nowadays, great efforts have been made to research self-powered devices that can work without consuming external power.[20–22] For example, self-powered PDs are highly desired for long-term unattended waste-water and air-pollution monitoring.[23] Zinc oxide (ZnO), a typical n-type transparent oxide semiconductor with a direct wide bandgap (3.37 eV), is one of the most important nanomaterials and a promising candidate in ultraviolet (UV) photodetection, benefiting from its unique characteristics, such as high resistance to irradiation, low deposition temperature, and a rich variety of nanostructure forms.[24–26] P–n junctions are a widely adopted structure for photodetection. Since the efficient p-type doping of ZnO is still a huge challenge, ZnO has been combined with other available p-type materials to form a heterojunction. Among these available p-type materials, nickel oxide (NiO) has been highlighted for its intrinsic p-type conductivity and transparent oxide semiconductor nature.[27]

In this paper, UV PDs have been fabricated from n-ZnO/p-NiO core–shell nanowire (NW) arrays. The PDs can operate without an external power supply, and show a response only to a narrow spectrum range.

Experimental

The ZnO NW arrays were grown on a sapphire substrate in a metal-organic chemical vapor deposition technique without using any catalysts or buffer layers. Diethylzinc and oxygen were used as the precursors, and high-purity (7 N) nitrogen was employed as a carrier to lead the precursors into the growth chamber. The substrate temperature was fixed at 550 °C and the chamber pressure at 3000 Pa. The as-grown ZnO NWs show n-type conductivity with an electron concentration of about 1×10^{16} cm^{-3}. After that, a nickel oxide (NiO) layer was deposited on the ZnO NW arrays in a reactive radio-frequency magnetron sputtering technique using a 99.999% nickel target at a radio frequency power of 190 W. Finally, a semi-transparent Au layer and an In layer was deposited onto the NiO layer and ZnO NWs acting as electrodes, respectively, in a vacuum evaporation method.

The morphology of the ZnO NW arrays was characterized using a Hitachi S4800 field-emission scanning electron microscope (SEM). The electrical properties of the ZnO and NiO layers

[a]State Key Laboratory of Luminescence and Applications, Changchun Institute of Optics, Fine Mechanics and Physics, Chinese Academy of Sciences, Changchun 130033, China. E-mail: shancx@ciomp.ac.cn

[b]Graduate University of Chinese Academy of Sciences, Beijing 100049, China

were characterized using a Hall measurement system (Lake-Shore 7707). A Bruker-D8 X-ray diffractometer with Cu-Kα radiation (1.54 Å) was used to evaluate the crystalline properties of the layers. The optical absorption spectra of the layers were recorded using a Shimadzu UV-3101PC spectrophotometer. Photoluminescence (PL) measurements of the ZnO NW arrays were carried out under the excitation of a He–Cd laser (λ = 325 nm). The current–voltage (*I–V*) characteristics of the structures were measured using a Keithley 2611A power source. The photoresponse of the NiO/ZnO nanowire array based PDs was measured using a Xe lamp, monochromator, chopper, and lock-in amplifier at room temperature. The temporal response of the PDs was measured by employing a pulsed Nd:YAG laser (355 nm, 10 ns) as the excitation source.

Results and discussion

The cross-sectional SEM image of the as-grown ZnO NW arrays is shown in Fig. 1(a). Highly oriented vertical ZnO NWs with a diameter of about 30 nm have been prepared on the sapphire substrate. Six well-defined peaks with 60° intervals are clearly seen from the XRD phi-scan spectrum, as shown in Fig. 1(b), which indicates that the ZnO NWs have a 6-fold symmetry. To investigate the optical quality of the ZnO NWs, the PL spectra at both room temperature and 80 K were measured, as illustrated in Fig. 1(c) and (d). The ZnO NWs exhibit strong UV emission and almost no defect-related emission at room temperature, indicating their high optical quality. Furthermore, the high optical quality can also be verified by the dominant free exciton emissions at 80 K, as shown in Fig. 1(d), in which the peaks at 3.377 eV and 3.370 eV can be attributed to the type-B exciton (FX_B) and the type-A exciton (FX_A) emissions of ZnO, respectively.[28,29] Meanwhile, the peak at 3.354 eV may come from the bound exciton (BX) recombination, and the three peaks at 3.311 eV, 3.233 eV, and 3.164 eV can be attributed to the longitudinal optical (LO) phonon replicas of free excitons.[28–30]

To fabricate the core–shell p–n junction based UV PDs, a NiO shell layer was deposited onto the ZnO NWs. The surface and cross-sectional SEM images of the sample after the deposition of the NiO layer are shown in Fig. 2(a) and (b). It can be seen that each ZnO NW has been fully covered by the NiO shell layer, forming ZnO/NiO core–shell NW arrays. However, the NiO shell layer tapers from the top to the bottom, which may be caused by the non-uniform coating of the NiO layer onto ZnO nanowires. The average thickness of the NiO layer is estimated to be about 45 nm. The existence of NiO is confirmed by the XRD pattern shown in Fig. 3(a), in which the peaks at 36.9° and 42.9° can be indexed to the diffractions from the (111) and (200) facet of cubic NiO, respectively. To determine the optical bandgap as well as the electrical properties of the NiO layer, NiO films have also been deposited directly on a sapphire substrate in the same growth process, and the optical absorption spectrum of which is shown in Fig. 3(b). From the plot of $(ahv)^2$ *vs.* hv (a and hv are the absorption coefficient and photon energy, respectively), the bandgap of the NiO film can be derived to be around 3.71 eV, as indicated in the inset of Fig. 3(b), which is in good agreement with the reported value (3.7 eV).[27] The Hall measurement indicates that the NiO films show p-type conductivity with a hole concentration of 1.3×10^{17} cm^{-3} and a Hall mobility of 0.9 cm^2 V^{-1} s^{-1}.

The schematic diagram and the photograph of the n-ZnO/p-NiO core–shell NW array PDs are shown in Fig. 4(a), and the *I–V* characteristics of the PDs under dark conditions are shown in Fig. 4(b). Significant rectification characteristics with a turn-on voltage of about 1.7 V can be observed from the *I–V* curve. The linear curves for both Au on NiO and In on ZnO, as shown in the inset of Fig. 4(b), reveal that good ohmic contacts have

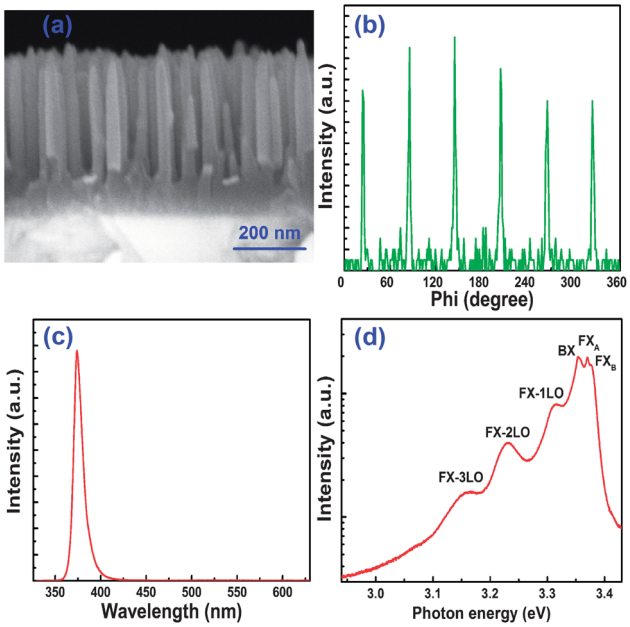

Fig. 1 The cross-sectional SEM image (a), XRD phi-scan pattern (b), PL spectrum at room temperature (c) and 80 K (d) of the as-grown ZnO NW arrays.

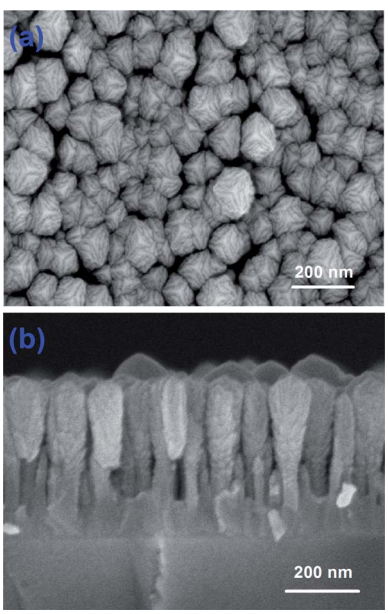

Fig. 2 The surface (a) and cross-sectional (b) SEM images of the ZnO/NiO core–shell NW arrays.

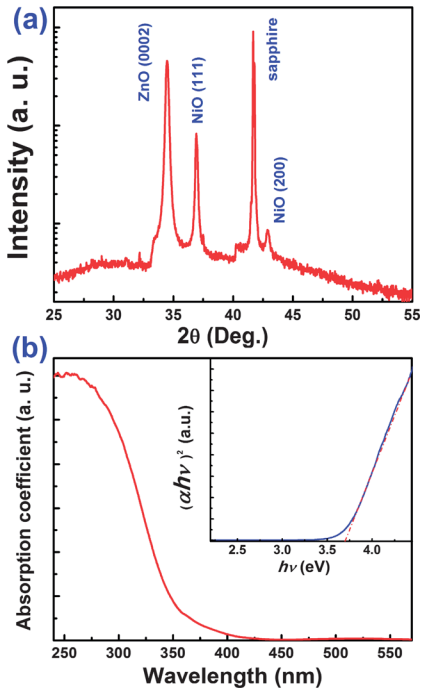

Fig. 3 (a) The XRD pattern of the ZnO/NiO core–shell NWs; (b) optical absorption spectrum of the NiO films and the inset shows a plot of $(ah\nu)^2$ *vs.* $h\nu$.

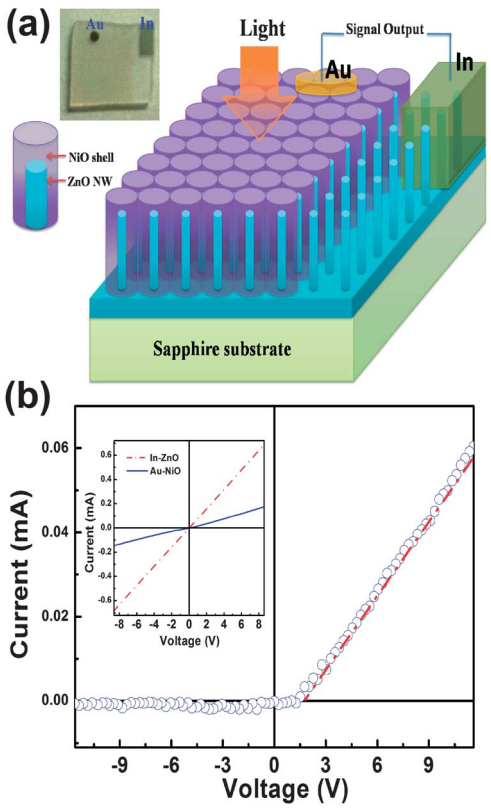

Fig. 4 (a) The schematic diagram and illumination geometry of the n-ZnO/p-NiO core–shell NW array PDs, and the inset shows the photograph of the device; (b) *I–V* characteristics of the PDs, and the inset shows the *I–V* curves of the Au electrode on the NiO and the In electrode on the ZnO layer.

been obtained in both electrodes. The ohmic behaviors of the metal contacts exclude the possibility of the formation of any Schottky junctions in the device, confirming that the rectification behavior arises from the n-ZnO/p-NiO interface.

Fig. 5 shows the response spectrum of the PDs under front illumination conditions at zero bias. It can be seen that only one peak centered at around 372 nm can be observed in this spectrum, and the full width at half maximum of the response spectrum is about 28 nm, which means that the PDs only respond to the photons with an energy in this narrow region. This characteristic makes the proposed PDs superior to other nanoscale semiconductor PDs, which usually show responses to a broad spectrum region,[17–19] and consequently are useful in sensing photons with wavelengths in a certain spectrum region. The mechanism for the highly selective responsivity can be understood as follows: In the n-ZnO/p-NiO structure, there will be two regions in the NiO shell layer of the PDs at zero bias, that is, a depletion region near the ZnO NW and a neutral region in the outer-layer of the NiO layer. The thickness of the depletion layer in the NiO can be estimated from the following formula:[31,32]

$$W(R) = W_0\left[1 + \frac{1}{6}\left(\frac{W_0}{R}\right) + \frac{1}{9}\left(\frac{W_0}{R}\right)^2 + \frac{103}{1080}\left(\frac{W_0}{R}\right)^3 + O\left(\frac{W_0}{R}\right)^4\right] \quad (1)$$

$$W_0 = \sqrt{\frac{2\varepsilon_s}{q}\left(\frac{N_A + N_D}{N_A N_D}\right)V_{bi}} \quad (2)$$

$$N_A W_p = N_D W_n \quad (3)$$

where $W(R)$ is the depletion length at the surface of a cylindrical nanostructure with a radius R, W_0 is the depletion length at a planar interface, V_{bi} is the potential barrier associated with the interface, ε_s is the dielectric constant, N_A is the acceptor concentration, N_D is the donor concentration, W_p is the depletion length in the p-type side and W_n is the depletion length in the n-type side. By inserting all the known parameters into eqn (1), the depletion thickness in the p-type NiO side can be

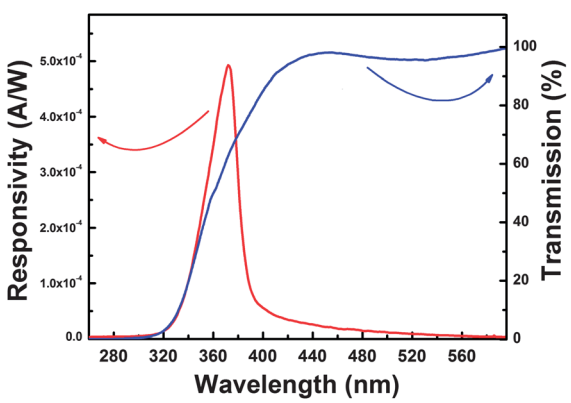

Fig. 5 The response spectrum of the PDs under front illumination conditions at zero bias and the transmission spectrum of the NiO films.

determined to be around 23 nm. Considering that the average thickness of the NiO shell is about 45 nm, the thickness of the neutral region in the NiO layer is around 22 nm. Since the penetration length of the photons is proportional to their wavelength, the photons with energy higher than the bandgap of NiO (3.71 eV) will be absorbed greatly by the neutral region of the NiO shell layer. Nevertheless, due to the small electric field in the neutral region, most of the photogenerated carriers in this region cannot reach the depletion region in the time scale of their lifetime, thus they will not contribute to the photoresponse of the PDs. As a result, the photons with short wavelengths will be filtered by the neutral region of the NiO shell layer, making the PDs highly spectrum-selective. To depict this "filter" function of the NiO shell layer more vividly, the transmission spectrum of the NiO film is shown in Fig. 5. As evidenced from the spectrum, the transmission of the NiO decreases quickly in the spectrum region shorter than 370 nm, and almost no photons with wavelengths shorter than 305 nm can pass through this layer. Furthermore, the peak responsivity of the PD at zero bias is about 0.493 mA W^{-1}. To our knowledge, this value is the highest currently reported result for p-NiO/n-ZnO heterojunction based PDs.[27,33,34] Meanwhile, it is over twice that of a p-GaN/n-ZnO nanoparticle wavelength-selective photodiode (0.225 mA W^{-1}),[35] and at least two orders of magnitude larger than that of an epitaxially grown p-GaN/n-ZnO heterojunction for selective UV detection (about 1.0×10^{-3} mA W^{-1}).[36]

Another advantage of the p–n type PDs is the fast response speed compared with the photoconductive PDs, of which the decay time is usually in the order of several seconds due to the presence of deep level traps and the adsorption of gas molecules (*e.g.* O_2, H_2O).[37–39] More recently, Dunn and co-workers reported a ZnO–nanorod/CuSCN PD with a decay time of 6.7 μs.[39] To test the response speed of our n-ZnO/p-NiO core–shell NW arrays UV PDs, the response rise time and the decay time of the structure were measured at zero bias and are shown in Fig. 6. The response time of the PDs is about 1.38 μs which is estimated as the 10–90% rise time. The decay edge can be well fitted to a second-order exponential decay function, with two time constants of 10.0 μs and 30.3 μs. This indicates that two channels may be responsible for the decay process, which has been widely found in ZnO NWs based PDs.[40,41] Although the detailed mechanisms are not clear yet, it shows that the decay time of the self-powered core–shell nanowire PDs is one of the fastest values ever reported for ZnO NW PDs.

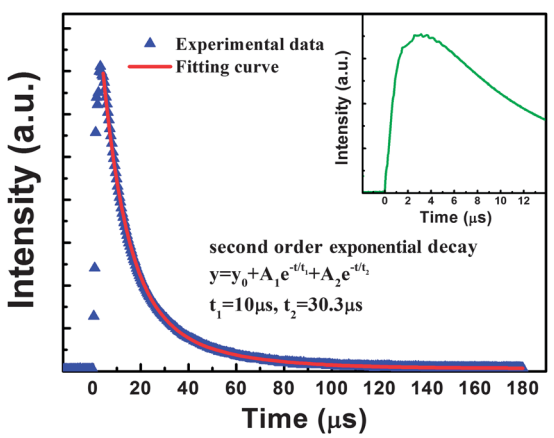

Fig. 6 The temporal response of the PDs at zero bias excited by Nd:YAG laser pulses and the inset shows the rise in the response.

Conclusions

In conclusion, self-powered, highly spectrum-selective UV PDs have been fabricated from n-ZnO/p-NiO core–shell NW arrays. The spectrum selectivity of the PDs is caused by the "filter" effect of the outer-layer of the p-NiO shell layer under front illustration conditions. The results reported in this paper may promise fast, spectrum-selective UV photodetection without power-consuming from ZnO-based nanowires.

Acknowledgements

This work was financially supported by the National Basic Research Program of China (2011CB302006), the Natural Science Foundation of China (11074248, 11104265, 11134009, and 61177040), and the Science and Technology Developing Project of Jilin Province (20111801).

Notes and references

1 X. H. Xia, J. P. Tu, Y. Q. Zhang, X. L. Wang, C. D. Gu, X. B. Zhao and H. J. Fan, *ACS Nano*, 2012, **6**, 5531–5538.
2 K. Wang, J. J. Chen, W. L. Zhou, Y. Zhang, Y. F. Yan, J. Pern and A. Mascarenhas, *Adv. Mater.*, 2008, **20**, 3248–3253.
3 Y. H. Wong and Q. Li, *J. Mater. Chem.*, 2004, **14**, 1413–1418.
4 J. A. Czaban, D. A. Thompson and R. R. LaPierre, *Nano Lett.*, 2009, **9**, 148–154.
5 J. Y. Tang, Z. Y. Huo, S. Brittman, H. W. Gao and P. D. Yang, *Nat. Nanotechnol.*, 2011, **6**, 568–572.
6 E. C. Garnett and P. D. Yang, *J. Am. Chem. Soc.*, 2008, **130**, 9224–9225.
7 B. S. Passmore, J. Wu, M. O. Manasreh, V. P. Kunets, P. M. Lytvyn and G. J. Salamo, *IEEE Electron Device Lett.*, 2008, **29**, 224–227.
8 M. Afsal, C. Y. Wang, L. W. Chu, H. Ouyang and L. J. Chen, *J. Mater. Chem.*, 2012, **22**, 8420–8425.
9 V. R. Reddy, J. Wu and M. O. Manasreh, *Mater. Lett.*, 2013, **92**, 296–299.
10 C. Cheng, T. L. Wang, L. Feng, W. Li, K. M. Ho, M. M. T. Loy, K. K. Fung and N. Wang, *Nanotechnology*, 2010, **21**, 475703.
11 Y. B. Tang, Z. H. Chen, H. S. Song, C. S. Lee, H. T. Cong, H. M. Cheng, W. J. Zhang, I. Bello and S. T. Lee, *Nano Lett.*, 2008, **8**, 4191–4195.
12 Y. Tak, S. J. Hong, J. S. Lee and K. Yong, *J. Mater. Chem.*, 2009, **19**, 5945–5951.
13 Z. X. Wang, X. Y. Zhan, Y. J. Wang, M. Safdar, M. Niu, J. P. Zhang, Y. Huang and J. He, *Appl. Phys. Lett.*, 2012, **101**, 073105.
14 L. Li, X. S. Fang, T. Y. Zhai, M. Y. Liao, U. K. Gautam, X. C. Wu, Y. Koide, Y. Bando and D. Golberg, *Adv. Mater.*, 2010, **22**, 4151–4156.

15 T. Y. Zhai, L. Li, X. Wang, X. S. Fang, Y. Bando and D. Golberg, *Adv. Funct. Mater.*, 2010, **20**, 4233–4248.
16 T. Y. Zhai, M. F. Ye, L. Li, X. S. Fang, M. Y. Liao, Y. F. Li, Y. Koide, Y. Bando and D. Golberg, *Adv. Mater.*, 2010, **22**, 4530–4533.
17 S. Panigrahi and D. Basak, *Nanoscale*, 2011, **3**, 2336.
18 C. L. Hsu and Y. C. Lu, *Nanoscale*, 2012, **4**, 5710.
19 H. Kang, J. Park, T. Choi, H. Jung, K. H. Lee, S. Im and H. Kim, *Appl. Phys. Lett.*, 2012, **100**, 041117.
20 S. Xu, Y. Qin, C. Xu, Y. Wei, R. Yang and Z. L. Wang, *Nat. Nanotechnol.*, 2010, **5**, 366–373.
21 Z. Y. Zhan, L. X. Zheng, Y. Z. Pan, G. Z. Sun and L. Li, *J. Mater. Chem.*, 2012, **22**, 2589–2595.
22 Y. Yang, W. Guo, J. J. Qi, J. Zhao and Y. Zhang, *Appl. Phys. Lett.*, 2010, **97**, 223113.
23 Q. Yang, Y. Liu, Z. Li, Z. Yang, X. Wang and Z. L. Wang, *Angew. Chem., Int. Ed.*, 2012, **124**, 1–5.
24 C. S. Lao, M. C. Park, Q. Kuang, Y. Deng, A. K. Sood, D. L. Polla and Z. L. Wang, *J. Am. Chem. Soc.*, 2007, **129**, 12096–12097.
25 Y. Z. Jin, J. P. Wang, B. Q. Sun, J. C. Blakesley and N. C. Greenham, *Nano Lett.*, 2008, **8**, 1649–1653.
26 A. M. Peiró, P. Ravirajan, K. Govender, D. S. Boyle, P. O'Brien, D. D. C. Bradley, J. Nelson and J. R. Durrant, *J. Mater. Chem.*, 2006, **16**, 2088–2096.
27 H. Ohta, M. Kamiya, T. Kamiya, M. Hirano and H. Hosono, *Thin Solid Films*, 2003, **445**, 317–321.
28 J. N. Dai, H. C. Liu, W. Q. Fang, L. Wang, Y. Pu, Y. F. Chen and F. Y. Jiang, *J. Cryst. Growth*, 2005, **283**, 93–99.
29 F. Y. Jiang, J. N. Dai, L. Wang, W. Q. Fang, Y. Pu, Q. M. Wang and Z. K. Tang, *J. Lumin.*, 2007, **122–123**, 162–164.
30 Y. Zhang, B. X. Lin, X. K. Sun and Z. X. Fu, *Appl. Phys. Lett.*, 2005, **86**, 131910.
31 J. H. Luscombe and C. L. Frenzen, *Solid-State Electron.*, 2002, **46**, 885–889.
32 S. M. Sze, *Physics of Semiconductor Devices*, John Wiley, New York, 2nd edn, 1981, p. 77.
33 S. Y. Tsai, M. H. Hon and Y. M. Lu, *Solid-State Electron.*, 2011, **63**, 37–41.
34 S. Y. Tsai, J. H. Lee and M. H. Hon, *Jpn. J. Appl. Phys.*, 2012, **51**, 06FE12.
35 L. Q. Qin, D. L. Shao, C. Shing and S. Sawyer, *Appl. Phys. Lett.*, 2013, **102**, 071106.
36 H. Zhu, C. X. Shan, B. Yao, B. H. Li, J. Y. Zhang, D. X. Zhao, D. Z. Shen and X. W. Fan, *J. Phys. Chem. C*, 2008, **112**, 20546–20548.
37 C. Soci, A. Zhang, B. Xiang, S. A. Dayeh, D. P. R. Aplin, J. Park, X. Y. Bao, Y. H. Lo and D. Wang, *Nano Lett.*, 2007, **7**, 1003–1009.
38 Y. Q. Bie, Z. M. Liao, H. Z. Zhang, G. R. Li, Y. Ye, Y. B. Zhou, J. Xu, Z. X. Qin, L. Dai and D. P. Yu, *Adv. Mater.*, 2011, **23**, 649–653.
39 S. M. Hatch, J. Briscoe and S. Dunn, *Adv. Mater.*, 2013, **25**, 867–871.
40 J. Zhou, Y. d. Gu, Y. F. Hu, W. J. Mai, P. H. Yeh, G. Bao, A. K. Sood, D. L. Polla and Z. L. Wang, *Appl. Phys. Lett.*, 2009, **94**, 191103.
41 R. Ghosh and D. Basak, *Appl. Phys. Lett.*, 2007, **90**, 243106.